Glance2Gaze: Efficient Vision-Language Models from Glance Fusion to Gaze Compression

Juan Chen[1,2]* **Honglin Liu**[2], **Yingying Ao**[2], **Ting Zhang**[3]† **Yan Huang**[1]†
Xudong Liu[2], **Biao Li**[2], **Jintao Fang**[2]

[1]School of Computer Science and Engineering, South China University of Technology
[2]Meituan Inc. [3]School of Artificial Intelligence, Beijing Normal University
`csjchen@mail.scut.edu.cn`, `tingzhang@bnu.edu.cn`, `aihuangy@scut.edu.cn`
`{liuhonglin03,aoyingying,liuxudong18,yaowenyuan,fangjintao}@meituan.com`

Abstract

Vision-language models heavily rely on visual representations, yet ensuring its efficiency remains a critical challenge. Most existing approaches focus on reducing visual tokens either at the visual encoder phase or during the LLM decoder stage. Inspired by human visual cognition, where an initial global glance precedes focused attention on semantically salient regions, we introduce Glance2Gaze, a cognitively inspired framework that mimics the human two-stage attention process. The framework consists of two key components: the Glance Fusion module, which integrates multi-layer vision transformer features with text-aware attention to generate a semantically enriched global representation, and the Gaze Compression module, which utilizes a novel query-guided mechanism to selectively compress visual tokens based on their semantic relevance. Experimental results on widely adopted benchmarks demonstrate that Glance2Gaze outperforms existing methods, achieving superior performance with equal or lower computational cost. Furthermore, it generalizes well to high-resolution and video scenarios, showcasing robust and scalable efficiency improvements in VLMs.

1 Introduction

Large Vision-Language Models (VLMs) [1–6] have made significant advances in image captioning, visual question answering, and multimodal dialogue understanding driven by the rapid progress of Large Language Models (LLMs) [7–11]. A typical VLM architecture consists of three key components: (i) a pre-trained visual encoder responsible for extracting dense image representations; (ii) a cross-modal projector that aligns visual features with textual embeddings; and (iii) a language model backbone that processes the combined visual-textual tokens to generate task-specific outputs. Central to this pipeline are visual tokens, whose quality critically impacts model performance and efficiency, making them a core focus in VLM design.

Visual tokens are conventionally extracted from images using pre-trained vision backbones such as CLIP-ViT [12], EVA [13], or InternImage [14], which generate fixed-length sequences of visual embeddings for downstream multimodal tasks. Recent advancements in large VLMs have shown that increasing the number of visual tokens can significantly improve performance by capturing finer visual details [4, 5, 15, 16]. However, denser visual token representations pose substantial computational challenges due to the quadratic complexity of attention mechanisms in LLMs, where

*This work was done when Juan Chen was an intern at Meituan Inc.
†Corresponding authors.

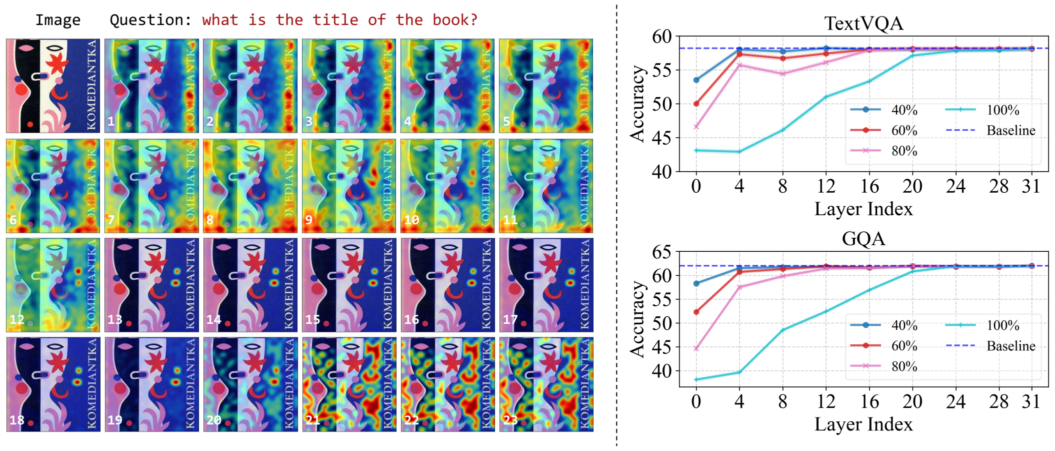

Figure 1: Left: Cross-modal attention heatmaps between instructions and visual tokens from different ViT layers, with numerical annotations indicating layer indices. Right: The pruning ratio-performance trade-off curve under LLaVA[3].

computational cost scales with the square of the total token count. Consequently, increasing token density exacerbates inference latency, memory consumption, and scalability issues.

In response to increasing complexity, substantial research has explored visual token selection, an approach that retains only the most informative tokens while discarding redundant or less relevant ones. This strategy is driven by the insight that not all visual tokens contribute equally to downstream tasks [17–23]. Existing methods can be broadly classified into two paradigms based on the stage at which pruning is applied. The first focuses on encoder-stage pruning [17, 19, 20, 22, 24], where token selection occurs within the visual encoder before fed into the language model. The second involves LLM-stage pruning [18, 21, 23, 25–27], where selection is performed alongside the language model decoder, often leveraging the full attention matrix to assess token importance. By selecting a subset of salient tokens, both paradigms aim to reduce token count while maintaining task performance, thereby enhancing computational efficiency. This paper also focus on efficient visual representation, providing novel insight from a cognitive perspective.

In this paper, we propose a novel framework for efficient vision-language models inspired by the glance-to-gaze mechanism observed in human visual cognition. Our work draws on the human eye movements that typically exhibit a two-stage pattern: initial fixations are broad and exploratory in nature, serving to rapidly acquire a global understanding of a scene, while subsequent fixations become increasingly focused [28]. Intuitively, human first perform a *glance* to capture the global layout and salient structures, followed by a *gaze* that zooms in on regions of interest for detailed inspection [29–32]. However, existing methods often aim to improve efficiency by selecting a subset of salient tokens, overlooking the hierarchical nature of human attention.

Motivated by this insight, we propose *Glance2Gaze*, a hierarchical visual token processing framework that emulates the dual-phase mechanism of rapid glancing followed by focused gazing. In contrast, our approach begins with a lightweight global scan to identify candidate regions and then progressively refines attention toward semantically rich subregions, enabling deeper cross-modal interaction. Specifically, Glance2Gaze comprises two complementary modules: Glance Fusion and Gaze Compression. Glance Fusion enables fast and holistic perception by dynamically aggregating multi-layer features rather than solely the penultimate ViT layer used in conventional approaches. We employ a text-aware attention to integrate hierarchical representations, enriching global semantics without increasing token count. As shown in Figure 1 (left), attention heatmaps across ViT layers indicate that each layer contributes distinctively to cross-modal understanding, highlighting the benefit of hierarchical feature aggregation for global context modeling. Building on the initial global understanding, Gaze Compression shifts the focus toward localized visual cues by progressively condensing visual tokens within the language model. This module is informed by the observation that token redundancy varies with decoding depth: shallow decoder layers are sensitive to pruning, whereas deeper layers remain robust under significant token reduction, as shown in Figure 1 (right).

We introduce a novel query-guided mechanism to selectively compress visual tokens based on their semantic relevance, facilitating a smooth transition from global to fine-grained visual reasoning.

We conduct extensive experiments to evaluate the effectiveness and efficiency of our proposed framework. Empirical results demonstrate that it consistently outperforms state-of-the-art baselines on both image and video understanding tasks, while maintaining comparable computational efficiency on the LLaVA backbone series. To ensure a comprehensive evaluation, we include a detailed analysis of computational cost, including inference latency comparison. Beyond empirical performance, our framework is grounded in cognitive principles drawn from human visual perception. By aligning model behavior with established cognitive mechanisms, our approach provides a principled, biologically inspired pathway toward more efficient vision-language models.

In summary, our key contributions are:

- We introduce a *Glance2Gaze*, a cognitively motivated two-stage visual token processing framework that mirrors human eye movement patterns, initial global glancing followed by focused gazing, to enhance efficiency in vision-language models.
- Building on the insight, we design a *Glance Fusion* module that aggregates multi-layer ViT features using text-aware attention, enriching global semantic understanding without increasing visual token count and a *Gaze Compression* module, an efficient iterative visual token compression method that uses a shared query pool to condense visual tokens, emulating the visual system's gaze process.
- We present an in-depth analysis about each component of the proposed framework. Empirically we demonstrate our approach delivers superior performance comparing with state-of-the-art baselines on both image understanding and video understanding tasks.

2 Related Work

Vision-Language models. Recent advances in LLMs like GPT [7] and LLaMA [9] have driven the emergence of VLMs [1–6, 33]. VLMs aim to process and understand information across multiple data modalities, including text, images, videos. LLaVA [2] pioneered open-source VLMs by introducing a visual-language instruction dataset and establishing a robust framework through the integration of CLIP-ViT-L-336px [12] visual encoder with the Vicuna [8] language model, thereby laying the groundwork for future architectures. However, it resizes each image into fixed number of visual tokens, hindering its performance in complex tasks. To enhance visual tokens, several methods [1, 4, 10, 15] have increased the number of image tokens to enhance model detail comprehension and reduce hallucinations. LLaVA-NeXT [15] dynamically divides images into patches, allowing the visual encoder to process them independently before concatenating them to form the visual representation. Meanwhile, Qwen2-VL [5] introduces dynamic resolution to accommodate high-resolution inputs and trains the visual encoder from scratch using extensive image-text pairs, resulting in improved performance on fine-grained tasks. Furthermore, video-based VLMs [34, 35] extract multiple frames to enhance video understanding, resulting in a substantial increase in token count. While increasing visual tokens aids in managing complex scenarios, the excessive volume can significantly hinder the practical application of VLMs in real-world settings. Recently, GG-Transformer [36] adopts a glance-and-gaze concept to improve the modeling of long-range dependencies and local contexts within ViTs. However, its objective differs fundamentally from ours, as it focuses on enhancing unimodal representational capacity in ViT, whereas our goal is to improve efficiency in VLM.

Visual compression for VLMs. Recent methods have concentrated on reducing the visual token count while aiming to preserve model performance. Prior works have explored compressing visual tokens before interfacing with the LLM [17, 19, 20, 22, 24, 33, 37, 38]. Resampler [39] utilizes a learnable query embedding to compress visual tokens from the vision encoder, while MQT [38] introduces random selection of queries to adapt token count to task needs. VisionZip [22] employs a training-free pruning strategy using encoder attention to identify and remove redundant tokens, similar to LLaVA-Prumerge [20]. These methods face challenges in optimizing performance and efficiency; excessive token retention leads to redundancy, whereas aggressive compression compromises accuracy. Another type of approaches [18, 21, 23, 25, 27] reduce token count in LLM decoders using attention matrices. FastV [18] proposes halving visual tokens post-second LLM layer, while SparseVLM [23] employs a training-free method to prune tokens based on text relevance scores. These rely on full attention matrices, making them incompatible with FlashAttn [40]. PDrop [21] attempts to address this by

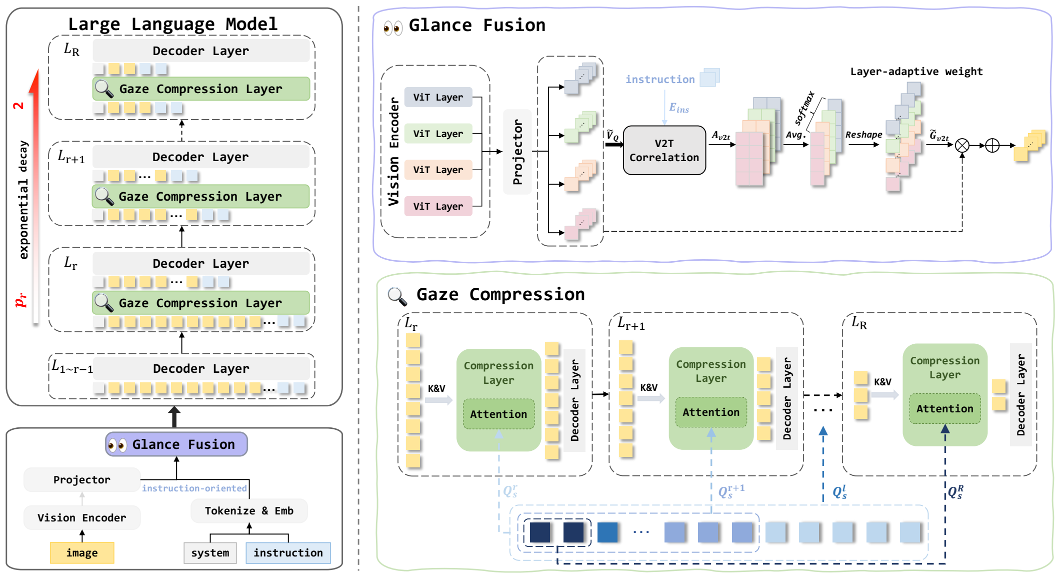

Figure 2: Diagram of the proposed Glance2Gaze framework. Glance Fusion combines hierarchical ViT features, guided by instruction, to produce enriched text-aware visual representations. Gaze Compression iteratively reduces visual tokens using a shared query embedding pool $\boldsymbol{Q}_s$.

introducing a lightweight similarity calculation before attention. However, these methods miss the human-like glance-to-gaze transition, which highlights the importance of capturing a global visual context before compression—a crucial aspect often neglected.

Unlike these methods, the proposed Glance2Gaze framework is inspired by cognitive principles and consists of two steps: Glance and Gaze, to efficiently compress visual tokens. The Glance step enhances overall image perception by providing additional detail, while the Gaze step gradually focuses on more relevant local areas with a novel query-guided compression.

3 Method

The Glance2Gaze architecture is depicted in Figure 2. Our design places the Glance Fusion module before the LLM and embeds the Gaze Compression module within it. Glance Fusion enhances text-aware visual representations by integrating ViT layers prior to token compression, while Gaze Compression iteratively reduces visual tokens starting at a specific decoder layer, transitioning focus from global scenes to local regions.

Revisiting VLMs. In VLMs, an image input $\boldsymbol{I} \in \mathbb{R}^{H\times W\times 3}$ is divided into N discrete tokens via patch convolution and refined through K transformer layers, yielding visual tokens $\boldsymbol{V} \in \mathbb{R}^{K\times N\times d_v}$, where d_v denotes the dimension of visual tokens. Typically, tokens from the penultimate layer are selected for input to the projector and subsequently the LLM. R denotes the total number of decoder layers in the LLM.

3.1 Glance Fusion

Building on the preceding analysis, we introduce Glance Fusion to enhance global context understanding. While prior studies [41–43] explored improving visual features using pre-trained visual encoders, these methods overlook the crucial interplay between textual and visual signals, thus limiting their performance gains. Dense Connector [41] divides ViT layers into groups, averages tokens within each group, and concatenates them across channels. MMFuser [42] utilizes deep ViT features as queries to retrieve missing details from shallow features. In contrast, Glance Fusion employs text-conditioned attention to dynamically integrates ViT's multi-level features, enabling task-aware feature weighting without incurring significant computational overhead or added token count.

Visual-instruction correlation. We first partition the ViT into distinct hierarchical stages to mitigate computational overhead while preserving representational diversity. We strategically sample intermediate layers from ViT. Let $\mathbb{L} = \{\boldsymbol{l}_1, \boldsymbol{l}_2, ..., \boldsymbol{l}_S\}$ denote the predefined set of layer indices (e.g., $\boldsymbol{l}_s \in [1, 24]$ for a 24-layer ViT), where $S = |\mathbb{L}|$ specifies the number of selected layers. From the full-layer image tokens $\boldsymbol{V} \in \mathbb{R}^{K \times N \times d_v}$, we extract tokens corresponding to $\mathbb{L}$, yielding a lightweight hierarchical representation $\tilde{\boldsymbol{V}} \in \mathbb{R}^{S \times N \times d_v}$. These tokens are then projected into the LLM's embedding space via the projector $\mathcal{P}_v$, yielding $\tilde{\boldsymbol{V}}_Q$:

$$\tilde{\boldsymbol{V}} = concat(\boldsymbol{V}_{\boldsymbol{l}_s}), \boldsymbol{l}_s \in \mathbb{L}, \tag{1}$$

$$\tilde{\boldsymbol{V}}_Q = \mathcal{P}_v(\tilde{\boldsymbol{V}}) \in \mathbb{R}^{S \times N \times d_t}, \tag{2}$$

where d_t denotes the dimension of text tokens.

Let T_{ins} denotes the input instruction tokens, we first generate its textual embedding $\boldsymbol{E}_{ins} \in \mathbb{R}^{M \times d_t}$ using the LLM's native embedding layer, ensuring parameter-sharing consistency with linguistic processing, M equals to the number of instruction tokens. To adaptively align textual semantics with hierarchical visual features, we introduce layer-specific projection layer $\{\mathcal{P}_t^s\}_{s=1}^S$, where $\mathcal{P}_t^s$ transforms $\boldsymbol{E}_{ins}$ into a subspace tailored for the $\tilde{\boldsymbol{V}}_Q^s$. Formally:

$$\boldsymbol{E}_{ins}^s = \mathcal{P}_t^s(\boldsymbol{E}_{ins}) \in \mathbb{R}^{M \times d_t}, s = 1, 2, ..., S. \tag{3}$$

For each layer $\boldsymbol{l}_s$, the projected text embedding $\boldsymbol{E}_{ins}^s$ is paired with its corresponding ViT feature $\tilde{\boldsymbol{V}}_Q^s$ to compute cross-modal correlation score, enabling granularity-aware fusion of visual semantics. Specifically, we take $\tilde{\boldsymbol{V}}_Q^s$ as query and $\boldsymbol{E}_{ins}^s$ as key to compute scaled dot-product correlation score, resulting in an attention matrix $\boldsymbol{A}_{v2t}^s \in \mathbb{R}^{N \times M}$. We calculate the row-wise average to form the vector $\boldsymbol{g}_{v2t}^s \in \mathbb{R}^N$, which represents the correlation of each image token in the $\boldsymbol{l}_s$-th ViT layer with all instruction tokens. Then we concatenate all $\boldsymbol{g}_{v2t}^s$ to form $\boldsymbol{G}_{v2t} \in \mathbb{R}^{S \times N}$:

$$\boldsymbol{A}_{v2t}^s = \frac{\tilde{\boldsymbol{V}}_Q^s \boldsymbol{E}_{ins}^{s\top}}{\sqrt{d_t}} \in \mathbb{R}^{N \times M}, s = 1, 2, ..., S, \tag{4}$$

$$\boldsymbol{g}_{v2t}^s = avg(\boldsymbol{A}_{v2t}^s) \in \mathbb{R}^N, s = 1, 2, ..., S, \tag{5}$$

$$\boldsymbol{G}_{v2t} = concat(\boldsymbol{g}_{v2t}^s) \in \mathbb{R}^{S \times N}. \tag{6}$$

Instruction-oriented integration. To optimally extract visual features that enhance instruction comprehension, we apply Softmax to $\boldsymbol{G}_{v2t}$ along the column dimension, yielding normalized correlation scores for each visual token across S different layers. These scores act as dynamic weights to produce task-enhanced visual tokens $\boldsymbol{V}_Q$, resulting in:

$$\tilde{\boldsymbol{G}}_{v2t} = softmax(\boldsymbol{G}_{v2t}, dim = 0), \tag{7}$$

$$\boldsymbol{V}_Q = \textstyle\sum_{s=1}^S \tilde{\boldsymbol{V}}_Q^s \odot \tilde{\boldsymbol{G}}_{v2t}^s \in \mathbb{R}^{N \times d_t}, \tag{8}$$

where $\odot$ denotes element-wise multiplication broadcasted along the token dimension. This method employs the correlation between instructions and ViT layers as weights to fuse their outputs, yielding task-enhanced visual features. These enhanced features, $\boldsymbol{V}_Q$, are then concatenated with text tokens for processing by the LLM.

3.2 Gaze Compression

We propose Gaze Compression, a parameter-efficient mechanism that iteratively reduces visual token count across decoder layers via a shared learnable query pool. Building on previous observation that shallow decoder layers are sensitive to pruning, we retain all visual tokens in the shallow decoder layers to fully understand them. Therefore, we decide to initiate the Gaze Compression from a predefined layer r. By retaining the full token count at shallow layers, we enable the LLM to thoroughly understand visual tokens and enhance overall comprehension, thus laying a solid foundation for subsequent compression.

Progressive gaze compression. To achieve token reduction, we define a monotonically decreasing sequence $P = [p_r, p_{r+1}, \ldots, p_R]$ with $p_r \geq p_{r+1} \geq \cdots \geq p_R$, where p_l $(r \leq l \leq R)$ represents the number of compressed visual tokens at the l-th decoder layer, which is less than the number of initial visual tokens, namely $p_r < N$. Starting from layer r, a query-based compression attention operation compresses visual tokens before they are inputted to each decoder layer. At each l-th layer in the LLM, a learnable query $\boldsymbol{Q}_l \in \mathbb{R}^{p_l \times d_t}$ is initialized, with visual tokens from l-1-th layer $\boldsymbol{H}_{l-1}$ serving as key and value for cross-attention computation. The attention output yields compressed visual tokens for the decoder layer's processing. However, distinct queries across layers increase parameter count and complicate optimization for discrete visual token extraction. To mitigate this, a learnable query embedding $\boldsymbol{Q}_s \in \mathbb{R}^{p_r \times d_t}$ is shared across all pertinent decoder layers. Consequently, at the l-th layer, the first p_l queries $\boldsymbol{Q}_s^l \in \mathbb{R}^{p_l \times d_t}$ are drawn from $\boldsymbol{Q}_s$, and visual tokens are compressed as follows:

$$\boldsymbol{H}_l = \mathcal{F}_o(softmax(\frac{\mathcal{F}_q(PE(\boldsymbol{Q}_s^l))\mathcal{F}_k(\boldsymbol{H}_{l-1})^\top}{\sqrt{d_t}})\mathcal{F}_v(\boldsymbol{H}_{l-1})), \tag{9}$$

where $\mathcal{F}_{o/q/k/v}$ denotes four distinct linear projection layers, and PE refers to the 2D Rotary Positional Embedding [10] applied to $\boldsymbol{Q}_s^l$ for spatial information perception. The resulting output $\boldsymbol{H}_l \in \mathbb{R}^{p_l \times d_t}$ replaces the input $\boldsymbol{H}_{l-1}$, yielding compressed visual tokens. By continually compressing beyond layer r, visual tokens are reduced, lowering computational demands in the decoder layers. This progressive reduction mimics the fine gazing process, focusing visual tokens on critical image regions.

3.3 Efficiency Analysis

Following prior work [21, 22], we report the FLOPs of the image token component. Glance Fusion accounts for less than 2.72% of the total FLOPs, which is therefore negligible compared to the computational cost incurred by visual token processing within LLM. We thus provide additional details in the supplementary material and here exclude it from further analysis.

Consequently, we focus solely on the FLOPs associated with the LLM's processing of visual tokens, evaluating efficiency from two perspectives: 1) the FLOPs required to process visual token sequences through decoder layers, and 2) the overhead introduced by Gaze Compression, as outlined in Eq. 9.

For Vicuna [8] (featuring 3-layer MLP following attention), the FLOPs per layer is $4n_l d_t^2 + 2n_l^2 d_t + 3n_l d_t d_m$, where n_l denotes the number of visual tokens ($n_l = N$ before layer r, $n_l = p_l$ thereafter) at l-th decoder layer and d_m is the hidden dimension of FFN. The compression overhead in Eq. 9 includes attention computation and four linear layers, resulting in $2(p_l d_t^2 + p_{l-1} d_t^2 + p_l p_{l-1} d_t)$ FLOPs, assuming $p_{l-1} = N$ when $l = r$. Then the overall computational cost is:

$$C = \sum_{l=1}^{R} 4n_l d_t^2 + 2n_l^2 d_t + 3n_l d_t d_m + \sum_{l=r}^{R} 2(p_l d_t^2 + p_{l-1} d_t^2 + p_l p_{l-1} d_t). \tag{10}$$

For instance, by setting r to 9 and using an exponentially decaying sequence $P = [256, \ldots, 2]$ in LLaVA-1.5-7B, we maintain only 33.2% of the FLOPs while minimally affecting performance across several benchmarks. To manage different compression ratios, p_R is always set to 2, with adjustments made to r and p_r. Additional details are provided in the supplementary material.

4 Experiments

4.1 Image Understanding Tasks

Benchmarks. To validate the effectiveness of our method in image understanding tasks, we conducted experiments on ten mainstream datasets, including TextVQA [44], POPE [45], GQA [46], VQAv2 [47], SEEDBench [48], MMBench [49], MME [50], ScienceQA-IMG [51], MMVet [52] and LLaVA-Bench-in-the-wild [2].

Implementation details. We applied the proposed method to both LLaVA-1.5-7B [3] and the high-resolution backbone, LLaVA-NeXT-7B [15], which increases the input image resolution to 4x more pixels. For LLaVA, the vision encoder was frozen while the remaining parameters were fine-tuned using the LLaVA-665k [3] dataset, adhering to the original training settings. For LLaVA-NeXT, all parameters were unfrozen during fine-tuning. Given its proprietary code and training data, we used the Open-LLaVA-NeXT [53], an open-source replication, for training, following PDrop [21]. In the

Table 1: The performance of Glance2Gaze at various compression configurations on LLaVA-1.5-7B, with FLOPs and the final column indicating the relative proportion of visual token computation and performance compared to the original model. **Bold** for best and underline for second-best performers.

Method	FLOPs	POPE	SQA	MME	GQA	SEED	MMB	VQAv2	TextVQA	MMVet	LLaVA-B	Avg.
LLaVA-1.5-7B	100%	85.9	69.5	1862	61.9	58.6	64.7	78.5	58.2	31.1	66.8	100%
FastV	33%	64.8	67.3	1612	52.7	57.1	61.2	67.1	52.5	27.7	49.4	87.5%
SparseVLM	33%	85.3	68.7	1787	59.5	58.7	64.1	75.6	57.8	**33.1**	66.1	99.0%
PDrop	33%	82.3	70.2	1766	57.1	54.7	63.2	-	56.1	30.5	-	96.2%
VisionZip	33%	84.9	68.2	**1834**	60.1	57.1	63.4	77.4	**57.8**	32.6	**66.7**	99.1%
Glance2Gaze	33%	**85.5**	**70.4**	1812	**61.5**	**58.7**	**64.5**	**77.6**	57.2	32.7	66.4	**99.9%**
FastV	22%	59.6	60.2	1490	49.6	55.9	56.1	61.8	50.6	28.1	52	83.2%
SparseVLM	22%	**85.0**	68.6	1746	58.4	**58.2**	**64.5**	73.8	56.7	29.0	62.7	96.3%
PDrop	22%	82.3	69.9	1664	56.0	53.3	61.1	-	55.1	30.8	-	94.4%
VisionZip	22%	83.7	68.3	**1823**	58.9	55.8	62.6	76.6	**57.0**	32.9	64.8	97.9%
Glance2Gaze	22%	84.5	**70.2**	1794	**59.3**	56.6	63.4	**77.4**	56.8	**33.1**	**65.4**	**98.7%**
FastV	11%	48.0	51.1	1256	46.1	51.9	48.0	55.0	47.8	25.8	46.1	73.8%
SparseVLM	11%	77.5	**69.8**	1589	53.8	52.2	60.1	68.2	53.4	24.9	57.5	89.0%
PDrop	11%	55.9	69.2	1092	41.9	40.0	33.3	-	45.9	30.7	-	73.5%
VisionZip	11%	80.9	68.8	**1756**	**57.0**	53.4	61.5	74.2	**56.0**	30.2	63.6	94.9%
Glance2Gaze	11%	**83.1**	69.1	1722	56.9	**53.9**	**61.7**	**74.9**	55.7	**31.4**	**64.1**	**95.6%**

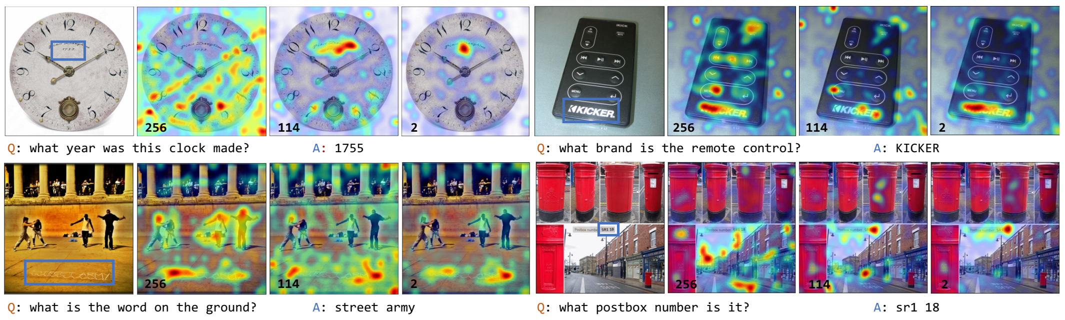
256
114
2
Q: what year was this clock made?
A: 1755
256
114
2
Q: what brand is the remote control?
A: KICKER
256
114
2
Q: what is the word on the ground?
A: street army
256
114
2
Q: what postbox number is it?
A: sr1 18

Figure 3: Visualization of different query embedding counts for compressing visual tokens from TextVQA [44]. Number within each image denotes p_l.

Glance Fusion module, $\mathbb{L}$ is set to {7, 13, 19, 23}. We implement the Gaze Compression strategy under different compression ratios. All experiments are conducted on 8 NVIDIA-A100-80G GPUs. Please refer to the supplementary material for more implementation details.

Results on LLaVA. Table 1 presents the performance of Glance2Gaze on LLaVA-1.5-7B [3], benchmarked against state-of-the-art approaches FastV [18], SparseVLM [23], PDrop [21], and VisionZip [22] across three FLOPs configurations, 33%, 22%, and 11%, indicating the computational ratio of visual processing compared to full token retention. Overall, Glance2Gaze consistently achieves top results at all compression levels and ranks as the best or second-best performer across nearly all datasets, showcasing its strong competitiveness. At 33% FLOPs, Glance2Gaze outperforms PDrop by 3.7% and VisionZip by 0.8%. Moreover, at 22% FLOPs, SparseVLM experience a 2.7% drop in accuracy, whereas Glance2Gaze only loses 1.2%, surpassing VisionZip by 0.8%. At the extreme compression ratio of 11%, Glance2Gaze retains 95.6% performance, exceeding VisionZip by 0.7% and SparseVLM by 6.6%, demonstrating its robust performance across various compression requirements.

Results on LLaVA-NEXT. LLaVA-NeXT extends LLaVA to handle high-resolution scenarios by dividing images into up to five patches, creating up to 2880 image tokens. Glance Fusion and Gaze Compression are applied independently to each sub-image. As shown in Table 2, Glance2Gaze exhibits greater advantages in high-resolution scenarios compared to standard resolutions. Glance2Gaze surpasses the second-best performer, VisionZip, with an average improvement of 1.2-1.3% across three FLOPs setting. Furthermore, Glance2Gaze surpasses VisionZip on nearly all datasets, demon-

Table 2: The performance of Glance2Gaze on LLaVA-NeXT-7B.

Method	FLOPs	TextVQA	POPE	SQA	MME	GQA	MMB	VQAv2	Avg.
LLaVA-NeXT-7B	100%	65.8	86.6	69.2	1801	63.8	67.2	80.5	100%
SparseVLM	22%	57.8	-	67.7	1772	60.3	65.7	77.1	95.4%
VisionZip	22%	60.8	87.6	67.9	1778	62.4	65.9	79.9	97.9%
Glance2Gaze	22%	**62.1**	**89.2**	**69.9**	**1784**	**63.1**	**66.4**	**80.1**	**99.2%**
SparseVLM	11%	55.9	-	67.3	1694	57.7	64.3	73.4	92.3%
VisionZip	11%	59.3	86.2	67.5	1770	61.0	**64.4**	78.4	96.3%
Glance2Gaze	11%	**60.5**	**87.5**	**69.9**	**1771**	**62.0**	64.3	**78.8**	**97.6%**
SparseVLM	5%	46.4	-	67.5	1542	51.2	63.1	66.3	85.0%
VisionZip	5%	57.3	83.4	67.5	1699	58.2	63.9	75.6	93.6%
Glance2Gaze	5%	**58.6**	**84.4**	**68.8**	**1718**	**58.9**	**64.0**	**76.4**	**94.8%**

Table 3: The performance of Glance2Gaze on Video-LLaVA at 6% FLOPs.

Method	TGIF	MSVD	MSRVTT	ActivityNet	Avg.
Video-LLaVA	47.1	69.8	56.7	43.1	100%
FastV	23.1	38.0	19.3	30.6	52.1%
SparseVLM	44.7	**68.2**	31.0	42.6	86.5%
VisionZip	42.4	63.5	52.1	43.0	93.2%
Glance2Gaze	**45.0**	66.5	**52.4**	**43.8**	**96.2%**

strating its robustness in preserving essential information during compression, especially in intricate OCR tasks such as TextVQA and VQAv2. The superior performance of Glance2Gaze in high-resolution scenarios likely stems from its ability to focus on spatially crucial details through the glance-to-gaze process, which becomes increasingly important as image complexity escalates.

4.2 Video Understanding Tasks

Benchmarks. Beyond image understanding, we applied the proposed method to video comprehension tasks, evaluating it on four widely adopted video-based question answering benchmarks: TGIF [54], MSVD [55], MSRVTT [55], and ActivityNet [56].

Implementation details. We use Video-LLaVA [34] to train a video VLM, which use Language Bind [57] as the vision encoder, extracts 8 frames from a video, encoding each into 256 visual tokens, culminating in 2048 image tokens in the end. To make a fair comparison with VisionZip and SparseVLM, r and p_r are set to 3 and 10 respectively to create a model with FLOPs reduced to 6% of the original. Please refer to supplementary material for more training details.

Performance on Video-LLaVA. In video understanding tasks, a substantial degree of frame-to-frame redundancy presents opportunities for computational efficiency without significantly compromising performance. Our method effectively capitalizes on this redundancy, achieving 96.2% of the performance using only 6% of FLOPs, whereas FastV suffers a 47.9% performance drop. Notably, Glance2Gaze outperforms VisionZip by 3% on average and ranks first on 3 out of 4 benchmarks, making it particularly suitable for real-time and large-scale video analysis applications.

4.3 Efficiency Comparison

Table 4 analyzes the computational costs, cuda time (i.e., the time required to generate the first token), overall latency (i.e., the total time to complete the entire sequence), and throughput on the TextVQA dataset, evaluated using a NVIDIA-A100-80G GPU, consistent across all compared baselines.

The results demonstrate that, under the same TFLOPs reduction ratio, Glance2Gaze not only delivers superior performance but also achieves the fastest inference speed, with a $6.39\times$ acceleration in prefilling time, a $3.15\times$ speedup in overall latency, and a $3.14\times$ improvement in throughput, effectively balancing efficiency and accuracy.

Table 4: Computational cost analysis comparison on LLaVA-NeXT-7B.

Method	TFLOPs	Cuda Time (ms)	Latency (ms)	Throughput	TextVQA
LLaVA-NeXT	53.83	313	475	10.884	65.8
FastV	2.76	170 (1.84×)	358 (1.33×)	12.272 (1.13×)	-
SparseVLM	2.76	183 (1.71×)	379 (1.25 ×)	13.233 (1.22×)	46.4
VisionZip	2.76	57 (5.49×)	192 (2.47×)	26.983 (2.48×)	57.3
Glance2Gaze	**2.67**	**49 (6.39×)**	**151 (3.15×)**	**34.121 (3.14×)**	**58.6**

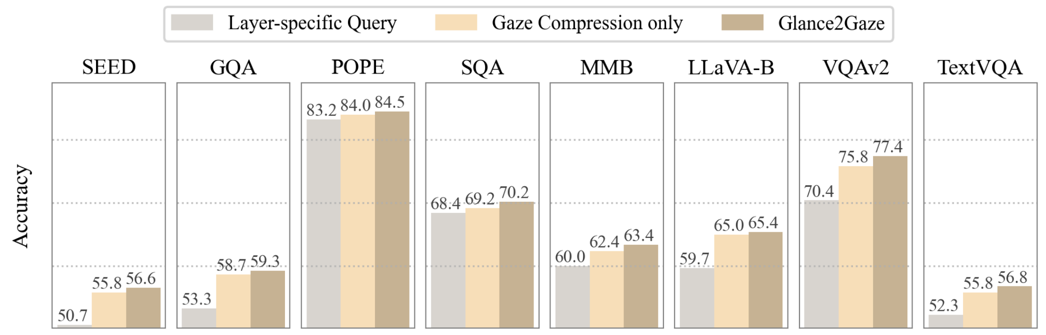

Figure 4: Ablation study evaluating the effect of a shared query pool in Gaze Compression comparing layer-specific query and the effect of Glance Fusion.

4.4 Analysis and Discussion

Visualization of Gaze Compression. Figure 3 illustrates the visual features learned by the query embedding at 33% FLOPs on TextVQA. Initially, with more visual tokens retained, the query captures broader global information. As compression progresses and fewer visual tokens are kept, focus shifts to regions containing the answer, demonstrating how the query learns to localize important areas through the gaze compression procedure, such as those involving text answers.

The effect of Gaze Compression compared to attention-based strategies. To rigorously assess the advantage of Gaze Compression over attention-based pruning, we evaluate both methods under an identical compression ratio. As shown in Table 5, attention-based pruning results in notable performance degradation. Even with subsequent fine-tuning, the baseline remains inferior to Glance2Gaze, underscoring that static pruning guided solely by local attention scores lacks the adaptability required for task-specific compression.

The effect of a shared query pool. We investigate the effects of using layer-specific queries in Gaze Compression, as shown in Figure 4. Using independent queries for each layer increases parameters and significantly damages performance across all datasets. This may be because the shared queries enhance pattern extraction from the same image, implicitly constraining the query's optimization domain. More ablations about Gaze Compression is available in the supplementary material.

The effect of Glance Fusion. Figure 4 demonstrates the impact of applying Gaze Compression alone and with Glance Fusion at 22% FLOPs on LLaVA-1.5-7B, resulting in substantial performance enhancements across all datasets. Notably, Glance Fusion improves accuracy by 1.0 and 1.6 points on TextVQA and VQAv2, respectively, where fine-grained image details are crucial for text understanding tasks. We emphasize that the additional computational overhead introduced by Glance Fusion is minimal, yet its effectiveness is substantial. More ablations about Glance Fusion is available in the supplementary material.

Comparison with other fusion strategies. We compare Glance Fusion with two representative fusion strategies, Dense Connector [41] and MMFuser [42], on LLaVA [3] with different scales, as summarized in Table 6. Dense Connector was not evaluated on LLaVA-1.5-13B and is therefore excluded from that setting. Glance Fusion consistently outperforms both baselines across model scales. On LLaVA-1.5-7B, it exceeds Dense Connector by 0.1–1.1 points, despite using fewer ViT layers (4 vs. 24), and surpasses MMFuser, which uses five layers, by 0.5–1.9 points. Similar

Table 5: Comparison of Gaze Compression with attention-based pruning methods.

Method	POPE	SQA	MME	GQA	SEED	MMB	VQAv2	TextVQA	MMVet	LLaVA-B	Avg.
w/o finetune	83.4	69.1	1775	59.7	54.7	63.0	74.6	55.8	30.6	62.0	96.1%
w finetune	84.7	69.1	1793	60.8	56.8	63.2	75.7	56.4	31.4	65.2	97.9%
Glance2Gaze	85.5	70.4	1812	61.5	58.7	64.5	77.6	57.2	32.7	66.4	99.9%

Table 6: Exploring the potential of Glance Fusion compared with other fusion strategies.

Method	GQA	VQAv2	SQA	TextVQA	POPE
LLaVA-7B	62.0	78.5	66.8	58.2	85.9
+Dense Connector	$63.8^{1.8\uparrow}$	$79.5^{1.0\uparrow}$	$69.5^{2.7\uparrow}$	$59.2^{1.0\uparrow}$	$86.6^{0.7\uparrow}$
+MMFuser	$62.8^{0.8\uparrow}$	$79.1^{0.6\uparrow}$	$68.7^{1.9\uparrow}$	$58.8^{0.6\uparrow}$	$86.3^{0.4\uparrow}$
+Glance Fusion	$64.1^{2.1\uparrow}$	$79.6^{1.1\uparrow}$	$70.6^{3.8\uparrow}$	$59.4^{1.2\uparrow}$	$87.2^{1.3\uparrow}$
LLaVA-13B	63.3	80.0	71.6	61.3	85.9
+MMFuser	$63.4^{0.1\uparrow}$	$80.1^{0.1\uparrow}$	$71.2^{0.4\downarrow}$	$59.9^{0.4\downarrow}$	$87.5^{1.6\uparrow}$
+Glance Fusion	$64.5^{1.2\uparrow}$	$80.4^{0.4\uparrow}$	$71.9^{0.3\uparrow}$	$61.8^{0.5\uparrow}$	$87.2^{1.3\uparrow}$

improvements are observed on LLaVA-1.5-13B. These results highlight Glance Fusion's superiority over task-agnostic fusion methods.

5 Conclusion and Limitation

This paper introduces a novel cognitive-inspired visual token compression through a two-stage *glance-to-gaze* approach. First, Glance Fusion dynamically merges multi-layer ViT features using a text-aware attention strategy to enhance image understanding. Next, Gaze Compression employs a query-based approach using a shared query pool to selectively compress visual tokens within LLM, mimicking the gaze process by progressively focusing on detailed local regions. Experimental results show that Glance2Gaze surpasses existing methods in performance with equal or reduced computational cost. While the overall framework is cognitively inspired, the internal mechanisms, particularly the fusion and compression strategies, remain largely heuristic and lack explicit modeling of cognitive processes. Future work could explore tighter integration with cognitive theories to further enhance both interpretability and performance.

Acknowledgments

This work was supported by the National Key Research and Development Program of China under Grant 2024YFE0105400, the Guangdong Provincial Key Field R&D Program under Grant 2024B0101040008, and the Guangzhou Science and Technology Plan Project – Key R&D Plan under Grant 2024B01W0007. This work was jointly supported by the Fundamental Research Funds for the Central Universities under Grant 2243100004 and 2253500001.

References

[1] Zhe Chen, Jiannan Wu, Wenhai Wang, Weijie Su, Guo Chen, Sen Xing, Muyan Zhong, Qinglong Zhang, Xizhou Zhu, Lewei Lu, et al. Internvl: Scaling up vision foundation models and aligning for generic visual-linguistic tasks. In *Proceedings of the IEEE/CVF conference on computer vision and pattern recognition*, pages 24185–24198, 2024.

[2] Haotian Liu, Chunyuan Li, Qingyang Wu, and Yong Jae Lee. Visual instruction tuning. *Advances in neural information processing systems*, 36:34892–34916, 2023.

[3] Haotian Liu, Chunyuan Li, Yuheng Li, and Yong Jae Lee. Improved baselines with visual instruction tuning. In *Proceedings of the IEEE/CVF Conference on Computer Vision and Pattern Recognition*, pages 26296–26306, 2024.

[4] Gemini Team, Rohan Anil, Sebastian Borgeaud, Jean-Baptiste Alayrac, Jiahui Yu, Radu Soricut, Johan Schalkwyk, Andrew M Dai, Anja Hauth, Katie Millican, et al. Gemini: a family of highly capable multimodal models. *arXiv preprint arXiv:2312.11805*, 2023.

[5] Peng Wang, Shuai Bai, Sinan Tan, Shijie Wang, Zhihao Fan, Jinze Bai, Keqin Chen, Xuejing Liu, Jialin Wang, Wenbin Ge, et al. Qwen2-vl: Enhancing vision-language model's perception of the world at any resolution. *arXiv preprint arXiv:2409.12191*, 2024.

[6] Deyao Zhu, Jun Chen, Xiaoqian Shen, Xiang Li, and Mohamed Elhoseiny. Minigpt-4: Enhancing vision-language understanding with advanced large language models. *arXiv preprint arXiv:2304.10592*, 2023.

[7] Josh Achiam, Steven Adler, Sandhini Agarwal, Lama Ahmad, Ilge Akkaya, Florencia Leoni Aleman, Diogo Almeida, Janko Altenschmidt, Sam Altman, Shyamal Anadkat, et al. Gpt-4 technical report. *arXiv preprint arXiv:2303.08774*, 2023.

[8] Wei-Lin Chiang, Zhuohan Li, Zi Lin, Ying Sheng, Zhanghao Wu, Hao Zhang, Lianmin Zheng, Siyuan Zhuang, Yonghao Zhuang, Joseph E Gonzalez, et al. Vicuna: An open-source chatbot impressing gpt-4 with 90%* chatgpt quality, march 2023. *URL https://lmsys. org/blog/2023-03-30-vicuna*, 3(5), 2023.

[9] Hugo Touvron, Thibaut Lavril, Gautier Izacard, Xavier Martinet, Marie-Anne Lachaux, Timothée Lacroix, Baptiste Rozière, Naman Goyal, Eric Hambro, Faisal Azhar, et al. Llama: Open and efficient foundation language models. *arXiv preprint arXiv:2302.13971*, 2023.

[10] An Yang, Baosong Yang, Beichen Zhang, Binyuan Hui, Bo Zheng, Bowen Yu, Chengyuan Li, Dayiheng Liu, Fei Huang, Haoran Wei, et al. Qwen2. 5 technical report. *arXiv preprint arXiv:2412.15115*, 2024.

[11] Susan Zhang, Stephen Roller, Naman Goyal, Mikel Artetxe, Moya Chen, Shuohui Chen, Christopher Dewan, Mona Diab, Xian Li, Xi Victoria Lin, et al. Opt: Open pre-trained transformer language models. *arXiv preprint arXiv:2205.01068*, 2022.

[12] Alec Radford, Jong Wook Kim, Chris Hallacy, Aditya Ramesh, Gabriel Goh, Sandhini Agarwal, Girish Sastry, Amanda Askell, Pamela Mishkin, Jack Clark, et al. Learning transferable visual models from natural language supervision. In *International conference on machine learning*, pages 8748–8763. PmLR, 2021.

[13] Quan Sun, Yuxin Fang, Ledell Wu, Xinlong Wang, and Yue Cao. Eva-clip: Improved training techniques for clip at scale. *arXiv preprint arXiv:2303.15389*, 2023.

[14] Wenhai Wang, Jifeng Dai, Zhe Chen, Zhenhang Huang, Zhiqi Li, Xizhou Zhu, Xiaowei Hu, Tong Lu, Lewei Lu, Hongsheng Li, et al. Internimage: Exploring large-scale vision foundation models with deformable convolutions. In *Proceedings of the IEEE/CVF conference on computer vision and pattern recognition*, pages 14408–14419, 2023.

[15] Haotian Liu, Chunyuan Li, Yuheng Li, Bo Li, Yuanhan Zhang, Sheng Shen, and Yong Jae Lee. Llava-next: Improved reasoning, ocr, and world knowledge, January 2024.

[16] Pan Zhang, Xiaoyi Dong, Bin Wang, Yuhang Cao, Chao Xu, Linke Ouyang, Zhiyuan Zhao, Haodong Duan, Songyang Zhang, Shuangrui Ding, et al. Internlm-xcomposer: A vision-language large model for advanced text-image comprehension and composition. *arXiv preprint arXiv:2309.15112*, 2023.

[17] Daniel Bolya, Cheng-Yang Fu, Xiaoliang Dai, Peizhao Zhang, Christoph Feichtenhofer, and Judy Hoffman. Token merging: Your vit but faster. *arXiv preprint arXiv:2210.09461*, 2022.

[18] Liang Chen, Haozhe Zhao, Tianyu Liu, Shuai Bai, Junyang Lin, Chang Zhou, and Baobao Chang. An image is worth 1/2 tokens after layer 2: Plug-and-play inference acceleration for large vision-language models. In *European Conference on Computer Vision*, pages 19–35. Springer, 2024.

[19] Ting Liu, Liangtao Shi, Richang Hong, Yue Hu, Quanjun Yin, and Linfeng Zhang. Multi-stage vision token dropping: Towards efficient multimodal large language model. *arXiv preprint arXiv:2411.10803*, 2024.

[20] Yuzhang Shang, Mu Cai, Bingxin Xu, Yong Jae Lee, and Yan Yan. Llava-prumerge: Adaptive token reduction for efficient large multimodal models. *arXiv preprint arXiv:2403.15388*, 2024.

[21] Long Xing, Qidong Huang, Xiaoyi Dong, Jiajie Lu, Pan Zhang, Yuhang Zang, Yuhang Cao, Conghui He, Jiaqi Wang, Feng Wu, et al. Pyramiddrop: Accelerating your large vision-language models via pyramid visual redundancy reduction. *arXiv preprint arXiv:2410.17247*, 2024.

[22] Senqiao Yang, Yukang Chen, Zhuotao Tian, Chengyao Wang, Jingyao Li, Bei Yu, and Jiaya Jia. Visionzip: Longer is better but not necessary in vision language models. *arXiv preprint arXiv:2412.04467*, 2024.

[23] Yuan Zhang, Chun-Kai Fan, Junpeng Ma, Wenzhao Zheng, Tao Huang, Kuan Cheng, Denis Gudovskiy, Tomoyuki Okuno, Yohei Nakata, Kurt Keutzer, et al. Sparsevlm: Visual token sparsification for efficient vision-language model inference. *arXiv preprint arXiv:2410.04417*, 2024.

[24] Shaolei Zhang, Qingkai Fang, Zhe Yang, and Yang Feng. Llava-mini: Efficient image and video large multimodal models with one vision token. *arXiv preprint arXiv:2501.03895*, 2025.

[25] Jieneng Chen, Luoxin Ye, Ju He, Zhao-Yang Wang, Daniel Khashabi, and Alan Yuille. Efficient large multi-modal models via visual context compression. In *The Thirty-eighth Annual Conference on Neural Information Processing Systems*, 2024.

[26] Wenxuan Huang, Zijie Zhai, Yunhang Shen, Shaosheng Cao, Fei Zhao, Xiangfeng Xu, Zheyu Ye, Yao Hu, and Shaohui Lin. Dynamic-llava: Efficient multimodal large language models via dynamic vision-language context sparsification. *arXiv preprint arXiv:2412.00876*, 2024.

[27] Weihao Ye, Qiong Wu, Wenhao Lin, and Yiyi Zhou. Fit and prune: Fast and training-free visual token pruning for multi-modal large language models. In *Proceedings of the AAAI Conference on Artificial Intelligence*, number 21, pages 22128–22136, 2025.

[28] Alfred L Yarbus. *Eye movements and vision*. Springer, 2013.

[29] Binh X Nguyen, Tuong Do, Huy Tran, Erman Tjiputra, Quang D Tran, and Anh Nguyen. Coarse-to-fine reasoning for visual question answering. In *Proceedings of the IEEE/CVF conference on computer vision and pattern recognition*, pages 4558–4566, 2022.

[30] EAB Over, ITC Hooge, BNS Vlaskamp, and CJ17617434 Erkelens. Coarse-to-fine eye movement strategy in visual search. *Vision Research*, 47(17):2272–2280, 2007.

[31] Kirsten Petras, Sanne Ten Oever, Christianne Jacobs, and Valerie Goffaux. Coarse-to-fine information integration in human vision. *NeuroImage*, 186:103–112, 2019.

[32] RJ Watt. Scanning from coarse to fine spatial scales in the human visual system after the onset of a stimulus. *Journal of the Optical Society of America A*, 4(10):2006–2021, 1987.

[33] Junnan Li, Dongxu Li, Silvio Savarese, and Steven Hoi. Blip-2: Bootstrapping language-image pre-training with frozen image encoders and large language models. In *International conference on machine learning*, pages 19730–19742. PMLR, 2023.

[34] Bin Lin, Bin Zhu, Yang Ye, Munan Ning, Peng Jin, and Li Yuan. Video-llava: Learning united visual representation by alignment before projection. *arXiv preprint arXiv:2311.10122*, 2023.

[35] Bin Lin, Zhenyu Tang, Yang Ye, Jiaxi Cui, Bin Zhu, Peng Jin, Jinfa Huang, Junwu Zhang, Yatian Pang, Munan Ning, et al. Moe-llava: Mixture of experts for large vision-language models. *arXiv preprint arXiv:2401.15947*, 2024.

[36] Qihang Yu, Yingda Xia, Yutong Bai, Yongyi Lu, Alan L Yuille, and Wei Shen. Glance-and-gaze vision transformer. *Advances in Neural Information Processing Systems*, 34:12992–13003, 2021.

[37] Wentong Li, Yuqian Yuan, Jian Liu, Dongqi Tang, Song Wang, Jie Qin, Jianke Zhu, and Lei Zhang. Tokenpacker: Efficient visual projector for multimodal llm. *arXiv preprint arXiv:2407.02392*, 2024.

[38] Wenbo Hu, Zi-Yi Dou, Liunian Li, Amita Kamath, Nanyun Peng, and Kai-Wei Chang. Matryoshka query transformer for large vision-language models. *Advances in Neural Information Processing Systems*, 37:50168–50188, 2024.

[39] Jean-Baptiste Alayrac, Jeff Donahue, Pauline Luc, Antoine Miech, Iain Barr, Yana Hasson, Karel Lenc, Arthur Mensch, Katherine Millican, Malcolm Reynolds, et al. Flamingo: a visual language model for few-shot learning. *Advances in neural information processing systems*, 35:23716–23736, 2022.

[40] Tri Dao, Dan Fu, Stefano Ermon, Atri Rudra, and Christopher Ré. Flashattention: Fast and memory-efficient exact attention with io-awareness. *Advances in neural information processing systems*, 35:16344–16359, 2022.

[41] Huanjin Yao, Wenhao Wu, Taojiannan Yang, YuXin Song, Mengxi Zhang, Haocheng Feng, Yifan Sun, Zhiheng Li, Wanli Ouyang, and Jingdong Wang. Dense connector for mllms. *Advances in Neural Information Processing Systems*, 37:33108–33140, 2024.

[42] Yue Cao, Yangzhou Liu, Zhe Chen, Guangchen Shi, Wenhai Wang, Danhuai Zhao, and Tong Lu. Mmfuser: Multimodal multi-layer feature fuser for fine-grained vision-language understanding. *arXiv preprint arXiv:2410.11829*, 2024.

[43] Gongwei Chen, Leyang Shen, Rui Shao, Xiang Deng, and Liqiang Nie. Lion: Empowering multimodal large language model with dual-level visual knowledge. In *Proceedings of the IEEE/CVF Conference on Computer Vision and Pattern Recognition*, pages 26540–26550, 2024.

[44] Amanpreet Singh, Vivek Natarajan, Meet Shah, Yu Jiang, Xinlei Chen, Dhruv Batra, Devi Parikh, and Marcus Rohrbach. Towards vqa models that can read. In *Proceedings of the IEEE/CVF conference on computer vision and pattern recognition*, pages 8317–8326, 2019.

[45] Yifan Li, Yifan Du, Kun Zhou, Jinpeng Wang, Wayne Xin Zhao, and Ji-Rong Wen. Evaluating object hallucination in large vision-language models. *arXiv preprint arXiv:2305.10355*, 2023.

[46] Drew A Hudson and Christopher D Manning. Gqa: A new dataset for real-world visual reasoning and compositional question answering. In *Proceedings of the IEEE/CVF conference on computer vision and pattern recognition*, pages 6700–6709, 2019.

[47] Yash Goyal, Tejas Khot, Douglas Summers-Stay, Dhruv Batra, and Devi Parikh. Making the v in vqa matter: Elevating the role of image understanding in visual question answering. In *Proceedings of the IEEE conference on computer vision and pattern recognition*, pages 6904–6913, 2017.

[48] Bohao Li, Rui Wang, Guangzhi Wang, Yuying Ge, Yixiao Ge, and Ying Shan. Seed-bench: Benchmarking multimodal llms with generative comprehension. *arXiv preprint arXiv:2307.16125*, 2023.

[49] Yuan Liu, Haodong Duan, Yuanhan Zhang, Bo Li, Songyang Zhang, Wangbo Zhao, Yike Yuan, Jiaqi Wang, Conghui He, Ziwei Liu, et al. Mmbench: Is your multi-modal model an all-around player? In *European conference on computer vision*, pages 216–233. Springer, 2024.

[50] Chaoyou Fu, Peixian Chen, Yunhang Shen, Yulei Qin, Mengdan Zhang, Xu Lin, Jinrui Yang, Xiawu Zheng, Ke Li, Xing Sun, Yunsheng Wu, and Rongrong Ji. Mme: A comprehensive evaluation benchmark for multimodal large language models, 2024.

[51] Pan Lu, Swaroop Mishra, Tanglin Xia, Liang Qiu, Kai-Wei Chang, Song-Chun Zhu, Oyvind Tafjord, Peter Clark, and Ashwin Kalyan. Learn to explain: Multimodal reasoning via thought chains for science question answering. *Advances in Neural Information Processing Systems*, 35:2507–2521, 2022.

[52] Weihao Yu, Zhengyuan Yang, Linjie Li, Jianfeng Wang, Kevin Lin, Zicheng Liu, Xinchao Wang, and Lijuan Wang. Mm-vet: Evaluating large multimodal models for integrated capabilities. *arXiv preprint arXiv:2308.02490*, 2023.

[53] Lin Chen and Long Xing. Open-llava-next: An open-source implementation of llava-next series for facilitating the large multi-modal model community. `https://github.com/xiaoachen98/Open-LLaVA-NeXT`, 2024.

[54] Yunseok Jang, Yale Song, Youngjae Yu, Youngjin Kim, and Gunhee Kim. Tgif-qa: Toward spatio-temporal reasoning in visual question answering. In *Proceedings of the IEEE conference on computer vision and pattern recognition*, pages 2758–2766, 2017.

[55] Dejing Xu, Zhou Zhao, Jun Xiao, Fei Wu, Hanwang Zhang, Xiangnan He, and Yueting Zhuang. Video question answering via gradually refined attention over appearance and motion. In *Proceedings of the 25th ACM international conference on Multimedia*, pages 1645–1653, 2017.

[56] Fabian Caba Heilbron, Victor Escorcia, Bernard Ghanem, and Juan Carlos Niebles. Activitynet: A large-scale video benchmark for human activity understanding. In *Proceedings of the ieee conference on computer vision and pattern recognition*, pages 961–970, 2015.

[57] Bin Zhu, Bin Lin, Munan Ning, Yang Yan, Jiaxi Cui, HongFa Wang, Yatian Pang, Wenhao Jiang, Junwu Zhang, Zongwei Li, et al. Languagebind: Extending video-language pretraining to n-modality by language-based semantic alignment. *arXiv preprint arXiv:2310.01852*, 2023.

[58] Ruipu Luo, Ziwang Zhao, Min Yang, Junwei Dong, Da Li, Pengcheng Lu, Tao Wang, Linmei Hu, Minghui Qiu, and Zhongyu Wei. Valley: Video assistant with large language model enhanced ability. *arXiv preprint arXiv:2306.07207*, 2023.

NeurIPS Paper Checklist

1. **Claims**

   Question: Do the main claims made in the abstract and introduction accurately reflect the paper's contributions and scope?

   Answer: [Yes]

   Justification: The claims are consistent with the contributions and scope as detailed in the abstract and introduction.

   Guidelines:

   - The answer NA means that the abstract and introduction do not include the claims made in the paper.
   - The abstract and/or introduction should clearly state the claims made, including the contributions made in the paper and important assumptions and limitations. A No or NA answer to this question will not be perceived well by the reviewers.
   - The claims made should match theoretical and experimental results, and reflect how much the results can be expected to generalize to other settings.
   - It is fine to include aspirational goals as motivation as long as it is clear that these goals are not attained by the paper.

2. **Limitations**

   Question: Does the paper discuss the limitations of the work performed by the authors?

   Answer: [Yes]

   Justification: The limitations are discussed in Section 5.

   Guidelines:

   - The answer NA means that the paper has no limitation while the answer No means that the paper has limitations, but those are not discussed in the paper.
   - The authors are encouraged to create a separate "Limitations" section in their paper.
   - The paper should point out any strong assumptions and how robust the results are to violations of these assumptions (e.g., independence assumptions, noiseless settings, model well-specification, asymptotic approximations only holding locally). The authors should reflect on how these assumptions might be violated in practice and what the implications would be.
   - The authors should reflect on the scope of the claims made, e.g., if the approach was only tested on a few datasets or with a few runs. In general, empirical results often depend on implicit assumptions, which should be articulated.
   - The authors should reflect on the factors that influence the performance of the approach. For example, a facial recognition algorithm may perform poorly when image resolution is low or images are taken in low lighting. Or a speech-to-text system might not be used reliably to provide closed captions for online lectures because it fails to handle technical jargon.
   - The authors should discuss the computational efficiency of the proposed algorithms and how they scale with dataset size.
   - If applicable, the authors should discuss possible limitations of their approach to address problems of privacy and fairness.
   - While the authors might fear that complete honesty about limitations might be used by reviewers as grounds for rejection, a worse outcome might be that reviewers discover limitations that aren't acknowledged in the paper. The authors should use their best judgment and recognize that individual actions in favor of transparency play an important role in developing norms that preserve the integrity of the community. Reviewers will be specifically instructed to not penalize honesty concerning limitations.

3. **Theory assumptions and proofs**

   Question: For each theoretical result, does the paper provide the full set of assumptions and a complete (and correct) proof?

   Answer: [NA]

Justification: The paper does not include theoretical claim.

Guidelines:

- The answer NA means that the paper does not include theoretical results.
- All the theorems, formulas, and proofs in the paper should be numbered and cross-referenced.
- All assumptions should be clearly stated or referenced in the statement of any theorems.
- The proofs can either appear in the main paper or the supplemental material, but if they appear in the supplemental material, the authors are encouraged to provide a short proof sketch to provide intuition.
- Inversely, any informal proof provided in the core of the paper should be complemented by formal proofs provided in appendix or supplemental material.
- Theorems and Lemmas that the proof relies upon should be properly referenced.

4. **Experimental result reproducibility**

   Question: Does the paper fully disclose all the information needed to reproduce the main experimental results of the paper to the extent that it affects the main claims and/or conclusions of the paper (regardless of whether the code and data are provided or not)?

   Answer: [Yes]

   Justification: The experimental setup and datasets are detailed in Section 4, while the proposed architecture is clearly outlined in Section 3. The supplementary material includes comprehensive training parameters and recipes.

   Guidelines:

   - The answer NA means that the paper does not include experiments.
   - If the paper includes experiments, a No answer to this question will not be perceived well by the reviewers: Making the paper reproducible is important, regardless of whether the code and data are provided or not.
   - If the contribution is a dataset and/or model, the authors should describe the steps taken to make their results reproducible or verifiable.
   - Depending on the contribution, reproducibility can be accomplished in various ways. For example, if the contribution is a novel architecture, describing the architecture fully might suffice, or if the contribution is a specific model and empirical evaluation, it may be necessary to either make it possible for others to replicate the model with the same dataset, or provide access to the model. In general. releasing code and data is often one good way to accomplish this, but reproducibility can also be provided via detailed instructions for how to replicate the results, access to a hosted model (e.g., in the case of a large language model), releasing of a model checkpoint, or other means that are appropriate to the research performed.
   - While NeurIPS does not require releasing code, the conference does require all submissions to provide some reasonable avenue for reproducibility, which may depend on the nature of the contribution. For example
     (a) If the contribution is primarily a new algorithm, the paper should make it clear how to reproduce that algorithm.
     (b) If the contribution is primarily a new model architecture, the paper should describe the architecture clearly and fully.
     (c) If the contribution is a new model (e.g., a large language model), then there should either be a way to access this model for reproducing the results or a way to reproduce the model (e.g., with an open-source dataset or instructions for how to construct the dataset).
     (d) We recognize that reproducibility may be tricky in some cases, in which case authors are welcome to describe the particular way they provide for reproducibility. In the case of closed-source models, it may be that access to the model is limited in some way (e.g., to registered users), but it should be possible for other researchers to have some path to reproducing or verifying the results.

5. **Open access to data and code**

Question: Does the paper provide open access to the data and code, with sufficient instructions to faithfully reproduce the main experimental results, as described in supplemental material?

Answer: [No]

Justification: The data we used is open benchmarks which can be downloaded from their websites. Our code will be released upon paper's acceptance.

Guidelines:

- The answer NA means that paper does not include experiments requiring code.
- Please see the NeurIPS code and data submission guidelines (`https://nips.cc/public/guides/CodeSubmissionPolicy`) for more details.
- While we encourage the release of code and data, we understand that this might not be possible, so "No" is an acceptable answer. Papers cannot be rejected simply for not including code, unless this is central to the contribution (e.g., for a new open-source benchmark).
- The instructions should contain the exact command and environment needed to run to reproduce the results. See the NeurIPS code and data submission guidelines (`https://nips.cc/public/guides/CodeSubmissionPolicy`) for more details.
- The authors should provide instructions on data access and preparation, including how to access the raw data, preprocessed data, intermediate data, and generated data, etc.
- The authors should provide scripts to reproduce all experimental results for the new proposed method and baselines. If only a subset of experiments are reproducible, they should state which ones are omitted from the script and why.
- At submission time, to preserve anonymity, the authors should release anonymized versions (if applicable).
- Providing as much information as possible in supplemental material (appended to the paper) is recommended, but including URLs to data and code is permitted.

6. **Experimental setting/details**

   Question: Does the paper specify all the training and test details (e.g., data splits, hyperparameters, how they were chosen, type of optimizer, etc.) necessary to understand the results?

   Answer: [Yes]

   Justification: Detailed experimental settings are provided in Section 4 and supplementary materials.

   Guidelines:

   - The answer NA means that the paper does not include experiments.
   - The experimental setting should be presented in the core of the paper to a level of detail that is necessary to appreciate the results and make sense of them.
   - The full details can be provided either with the code, in appendix, or as supplemental material.

7. **Experiment statistical significance**

   Question: Does the paper report error bars suitably and correctly defined or other appropriate information about the statistical significance of the experiments?

   Answer: [No]

   Justification: Error bars are not reported because it would be computationally expensive.

   Guidelines:

   - The answer NA means that the paper does not include experiments.
   - The authors should answer "Yes" if the results are accompanied by error bars, confidence intervals, or statistical significance tests, at least for the experiments that support the main claims of the paper.
   - The factors of variability that the error bars are capturing should be clearly stated (for example, train/test split, initialization, random drawing of some parameter, or overall run with given experimental conditions).

- The method for calculating the error bars should be explained (closed form formula, call to a library function, bootstrap, etc.)
- The assumptions made should be given (e.g., Normally distributed errors).
- It should be clear whether the error bar is the standard deviation or the standard error of the mean.
- It is OK to report 1-sigma error bars, but one should state it. The authors should preferably report a 2-sigma error bar than state that they have a 96% CI, if the hypothesis of Normality of errors is not verified.
- For asymmetric distributions, the authors should be careful not to show in tables or figures symmetric error bars that would yield results that are out of range (e.g. negative error rates).
- If error bars are reported in tables or plots, The authors should explain in the text how they were calculated and reference the corresponding figures or tables in the text.

8. **Experiments compute resources**

   Question: For each experiment, does the paper provide sufficient information on the computer resources (type of compute workers, memory, time of execution) needed to reproduce the experiments?

   Answer: [Yes]

   Justification: The paper specifies the hardware used (8 NVIDIA-A100-80G GPUs) in Section 4. FLOPs and inference latency per test samples is provided, allowing for estimation of computational costs.

   Guidelines:

   - The answer NA means that the paper does not include experiments.
   - The paper should indicate the type of compute workers CPU or GPU, internal cluster, or cloud provider, including relevant memory and storage.
   - The paper should provide the amount of compute required for each of the individual experimental runs as well as estimate the total compute.
   - The paper should disclose whether the full research project required more compute than the experiments reported in the paper (e.g., preliminary or failed experiments that didn't make it into the paper).

9. **Code of ethics**

   Question: Does the research conducted in the paper conform, in every respect, with the NeurIPS Code of Ethics `https://neurips.cc/public/EthicsGuidelines`?

   Answer: [Yes]

   Justification: The research adheres to the NeurIPS Code of Ethics.

   Guidelines:

   - The answer NA means that the authors have not reviewed the NeurIPS Code of Ethics.
   - If the authors answer No, they should explain the special circumstances that require a deviation from the Code of Ethics.
   - The authors should make sure to preserve anonymity (e.g., if there is a special consideration due to laws or regulations in their jurisdiction).

10. **Broader impacts**

    Question: Does the paper discuss both potential positive societal impacts and negative societal impacts of the work performed?

    Answer: [Yes]

    Justification: Both positive and negative societal impacts are discussed in supplementary material.

    Guidelines:

    - The answer NA means that there is no societal impact of the work performed.
    - If the authors answer NA or No, they should explain why their work has no societal impact or why the paper does not address societal impact.

- Examples of negative societal impacts include potential malicious or unintended uses (e.g., disinformation, generating fake profiles, surveillance), fairness considerations (e.g., deployment of technologies that could make decisions that unfairly impact specific groups), privacy considerations, and security considerations.
- The conference expects that many papers will be foundational research and not tied to particular applications, let alone deployments. However, if there is a direct path to any negative applications, the authors should point it out. For example, it is legitimate to point out that an improvement in the quality of generative models could be used to generate deepfakes for disinformation. On the other hand, it is not needed to point out that a generic algorithm for optimizing neural networks could enable people to train models that generate Deepfakes faster.
- The authors should consider possible harms that could arise when the technology is being used as intended and functioning correctly, harms that could arise when the technology is being used as intended but gives incorrect results, and harms following from (intentional or unintentional) misuse of the technology.
- If there are negative societal impacts, the authors could also discuss possible mitigation strategies (e.g., gated release of models, providing defenses in addition to attacks, mechanisms for monitoring misuse, mechanisms to monitor how a system learns from feedback over time, improving the efficiency and accessibility of ML).

11. **Safeguards**

    Question: Does the paper describe safeguards that have been put in place for responsible release of data or models that have a high risk for misuse (e.g., pretrained language models, image generators, or scraped datasets)?

    Answer: [NA]

    Justification: The paper does not release high-risk data or models.

    Guidelines:

    - The answer NA means that the paper poses no such risks.
    - Released models that have a high risk for misuse or dual-use should be released with necessary safeguards to allow for controlled use of the model, for example by requiring that users adhere to usage guidelines or restrictions to access the model or implementing safety filters.
    - Datasets that have been scraped from the Internet could pose safety risks. The authors should describe how they avoided releasing unsafe images.
    - We recognize that providing effective safeguards is challenging, and many papers do not require this, but we encourage authors to take this into account and make a best faith effort.

12. **Licenses for existing assets**

    Question: Are the creators or original owners of assets (e.g., code, data, models), used in the paper, properly credited and are the license and terms of use explicitly mentioned and properly respected?

    Answer: [Yes]

    Justification: The paper properly cites the sources for existing methods and benchmarks and respect their CC-BY-SA Licenses.

    Guidelines:

    - The answer NA means that the paper does not use existing assets.
    - The authors should cite the original paper that produced the code package or dataset.
    - The authors should state which version of the asset is used and, if possible, include a URL.
    - The name of the license (e.g., CC-BY 4.0) should be included for each asset.
    - For scraped data from a particular source (e.g., website), the copyright and terms of service of that source should be provided.

- If assets are released, the license, copyright information, and terms of use in the package should be provided. For popular datasets, `paperswithcode.com/datasets` has curated licenses for some datasets. Their licensing guide can help determine the license of a dataset.
- For existing datasets that are re-packaged, both the original license and the license of the derived asset (if it has changed) should be provided.
- If this information is not available online, the authors are encouraged to reach out to the asset's creators.

13. **New assets**

    Question: Are new assets introduced in the paper well documented and is the documentation provided alongside the assets?

    Answer: [NA]

    Justification: No new assets are introduced in the paper.

    Guidelines:

    - The answer NA means that the paper does not release new assets.
    - Researchers should communicate the details of the dataset/code/model as part of their submissions via structured templates. This includes details about training, license, limitations, etc.
    - The paper should discuss whether and how consent was obtained from people whose asset is used.
    - At submission time, remember to anonymize your assets (if applicable). You can either create an anonymized URL or include an anonymized zip file.

14. **Crowdsourcing and research with human subjects**

    Question: For crowdsourcing experiments and research with human subjects, does the paper include the full text of instructions given to participants and screenshots, if applicable, as well as details about compensation (if any)?

    Answer: [NA]

    Justification: The research does not involve crowdsourcing experiments or research with human subjects.

    Guidelines:

    - The answer NA means that the paper does not involve crowdsourcing nor research with human subjects.
    - Including this information in the supplemental material is fine, but if the main contribution of the paper involves human subjects, then as much detail as possible should be included in the main paper.
    - According to the NeurIPS Code of Ethics, workers involved in data collection, curation, or other labor should be paid at least the minimum wage in the country of the data collector.

15. **Institutional review board (IRB) approvals or equivalent for research with human subjects**

    Question: Does the paper describe potential risks incurred by study participants, whether such risks were disclosed to the subjects, and whether Institutional Review Board (IRB) approvals (or an equivalent approval/review based on the requirements of your country or institution) were obtained?

    Answer: [NA]

    Justification: The paper does not involve research with human subjects.

    Guidelines:

    - The answer NA means that the paper does not involve crowdsourcing nor research with human subjects.
    - Depending on the country in which research is conducted, IRB approval (or equivalent) may be required for any human subjects research. If you obtained IRB approval, you should clearly state this in the paper.

- We recognize that the procedures for this may vary significantly between institutions and locations, and we expect authors to adhere to the NeurIPS Code of Ethics and the guidelines for their institution.
- For initial submissions, do not include any information that would break anonymity (if applicable), such as the institution conducting the review.

16. **Declaration of LLM usage**

    Question: Does the paper describe the usage of LLMs if it is an important, original, or non-standard component of the core methods in this research? Note that if the LLM is used only for writing, editing, or formatting purposes and does not impact the core methodology, scientific rigorousness, or originality of the research, declaration is not required.

    Answer: [Yes]

    Justification: The paper describes the usage of Vicuna [8] as a foundational component of the core method in this research, acknowledging its importance and originality. The authors have obtained the necessary authorization to use this model, ensuring compliance with relevant guidelines and respecting intellectual property rights. Hence, the use of Vicuna is integral to the methodology presented and is well-documented within the paper.

    Guidelines:

    - The answer NA means that the core method development in this research does not involve LLMs as any important, original, or non-standard components.
    - Please refer to our LLM policy (`https://neurips.cc/Conferences/2025/LLM`) for what should or should not be described.

A Supplementary Material

A.1 Broader Impact

The proposed Glance2Gaze advances vision-language models by introducing a cognitively inspired framework that harmonizes efficiency and performance through its two-stage attention mechanism. By mimicking human visual cognition—first capturing global context and then focusing on salient details—the method significantly reduces computational overhead while maintaining or improving accuracy across diverse tasks. This innovation broadens accessibility to advanced visual-language systems, enabling deployment in resource-limited settings such as edge devices or real-time applications. Its scalability to high-resolution and video inputs further extends practical utility in fields like medical imaging, autonomous systems, and multimedia analysis. Environmentally, the reduced computational demand aligns with sustainable AI development by lowering energy consumption. As a generalizable paradigm, Glance2Gaze also inspires future research in biologically inspired attention mechanisms, fostering interdisciplinary advancements in efficient multimodal learning.

A.2 Efficiency Analysis

Previous works [18, 21–23] typically measure efficiency by the computational cost of visual tokens in LLMs, a method we also adopt. Additionally, we analyze the extra computational load introduced by Glance Fusion.

FLOPs within Glance Fusion. Considering the computational cost incurred by Glance Fusion, we account for the FLOPs arising from all projection operations of both visual (Eq. 2) and textual (Eq. 3) inputs, as well as the overhead introduced by the visual-text correlation computation (Eq. 4). Specifically, the visual mapping introduces SNd_vd_t FLOPs, while the text mapping contributes SMd_t^2 FLOPs. Furthermore, the visual-text correlation involves S matrix multiplications, resulting in $SNMd_t$ FLOPs. Overall, the total FLOPs within the Glance Fusion module can be expressed as:

$$C_{glance} = SNd_vd_t + SMd_t^2 + SNMd_t. \tag{11}$$

FLOPs within LLM (Visual Tokens). We assess FLOPs of visual tokens within the LLM by examining two factors: (i) the standard forward pass through the decoder, and (ii) the additional cost introduced by the Gaze Compression module. For the visual token processing in Vicuna-7B [8], using a 3-layer MLP as FFN and 32 decoder layers, each layer incurs $4n_ld_t^2 + 2n_l^2d_t + 3n_ld_td_m$ FLOPs, where n_l and d_m denote the number of visual tokens and the hidden dimension of the FFN, respectively. In our framework, n_l is 576 before layer r and p_l thereafter, with l representing the LLM layer index. The FLOPs from Eq. 9 include 2 matrix multiplications and 4 linear projections, totaling $2p_{l-1}p_ld_t + 2p_{l-1}d_t^2 + 2p_ld_t^2$. Therefore, the total FLOPs within LLM are:

$$C_{llm} = \sum_{l=1}^{R} 4n_ld_t^2 + 2n_l^2d_t + 3n_ld_td_m + \sum_{l=r}^{R} 2(p_{l-1}p_ld_t + p_{l-1}d_t^2 + p_ld_t^2). \tag{12}$$

We found C_{glance} to be negligible compared to C_{llm}. For instance, in LLaVA-1.5-7B, with r set to 3 and p_r to 100, C_{llm} amounts to 1.1T FLOPs while C_{glance} is only 0.03T FLOPs, yielding a proportion of 0.0272. Given its insignificance, C_{glance} can be omitted from detailed computational analysis, allowing us to concentrate on the more impactful C_{llm} for performance assessment.

A.3 More Implementation Details

A.3.1 Image Understanding Tasks

Training Recipes. Following LLaVA [3], we employ a two-stage training strategy for Glance2Gaze. In the first stage, we align image-text pairs by retaining the LLaVA architecture and training only the projector on the LLaVA-558K dataset for one epoch with a batch size of 256 and a learning rate of 1e-3. In the second stage, we incorporate Glance Fusion and Gaze Compression into LLaVA, training all parameters except the visual encoder for one epoch with a batch size of 128 and a learning rate of 2e-5.

To train LLaVA-NeXT-7B [15], we employ Open-LLaVA-NeXT [53], an open-source replication, due to proprietary restrictions on the original code and training sets. Our approach involves a two-stage

Table 7: Compression configurations employed to LLaVA-1.5-7B.

FLOPs	r	P
33%	9	[256, 209, 170, 139, 114, 93, 76, 62, 50, 41, 33, 27, 22, 18, 15, 12, 10, 8, 6, 5, 4, 3, 2, 2]
22%	7	[121, 103, 88, 75, 64, 54, 46, 40, 34, 29, 24, 21, 18, 15, 13, 11, 9, 8, 7, 6, 5, 4, 3, 3, 2, 2]
11%	3	[100, 87, 77, 67, 59, 52, 45, 40, 35, 30, 27, 23, 20, 18, 16, 14, 12, 10, 9, 8, 7, 6, 5, 4, 4, 3, 3, 2, 2, 2]

Table 8: Compression configurations employed to LLaVA-NeXT-7B.

FLOPs	r	P
22%	7	[121, 103, 88, 75, 64, 54, 46, 40, 34, 29, 24, 21, 18, 15, 13, 11, 9, 8, 7, 6, 5, 4, 3, 3, 2, 2]
11%	3	[100, 87, 77, 67, 59, 52, 45, 40, 35, 30, 27, 23, 20, 18, 16, 14, 12, 10, 9, 8, 7, 6, 5, 4, 4, 3, 3, 2, 2, 2]
5%	2	[25, 23, 21, 19, 18, 16, 15, 14, 13, 12, 11, 10, 9, 8, 7, 7, 6, 6, 5, 5, 4, 4, 4, 3, 3, 3, 3, 2, 2, 2, 2]

training process. Similar to LLaVA-1.5-7B, the proposed Glance2Gaze is integrated only in the second stage. In the first stage, we focus solely on training the projector with a batch size of 256 and a learning rate of 1e-3 for one epoch using the LLaVA-558K dataset. In the second stage, Glance2Gaze is embedded into the LLaVA-NeXT architecture, with all parameters including the visual encoder unfrozen for training over two epochs with a batch size of 128 and a learning rate of 2e-5, utilizing the same dataset as in [53].

Implementation Details. In Glance Fusion, $\mathbb{L}$ is consistently set to $\{7, 13, 19, 23\}$ to capture fine-detailed features. For Gaze Compression, we adjust r and p_r to manage different computation configurations, as detailed in Table 7 and 8.

LLaVA-NeXT processes high-resolution images by dividing them into multiple sub-images (up to 5) for individual handling by the visual encoder, which are subsequently concatenated within the LLM. Both Glance Fusion and Gaze Compression are applied to each sub-image independently.

A.3.2 Video Understanding Tasks

Training Recipes. Following Video-LLaVA [34], we employ a two-stage training strategy. In the first stage, only the projector is trained for one epoch with a batch size of 256 and a learning rate of 1e-3, using the LLaVA-558K dataset and a subset of Valley [58], while retaining the original architecture. In the second stage, we integrate Glance Fusion and Gaze Compression into Video-LLaVA, freeze the vision encoder, and finetune all other parameters with a batch size of 128 and a learning rate of 2e-5, using the LLaVA-665K dataset and 100k video-text instructions from Video-ChatGPT [34].

Implementation Details. In Video-LLaVA [34], 8 frames are sampled from each video, with each frame encoded into 256 tokens, resulting in 2048 tokens per video. For Glance Fusion, $\mathbb{L}$ is set to $\{7, 13, 19, 23\}$ by default. Gaze Compression is applied to each frame, with $r = 3$ and $p_r = 10$, yielding a model that operates at 6% of the FLOPs required for full token retention.

A.3.3 More Ablation Studies

More ablation on the effect of a shared query pool. Figure 5 presents additional ablation results comparing layer-specific query embeddings with a shared query pool in Gaze Compression. While the layer-specific approach increases parameters, it significantly degrades performance across all datasets.

More ablation on the effect of Glance Fusion. To assess the importance of global glance fusion prior to gaze compression, we compare Gaze Compression alone with the full Glance2Gaze in

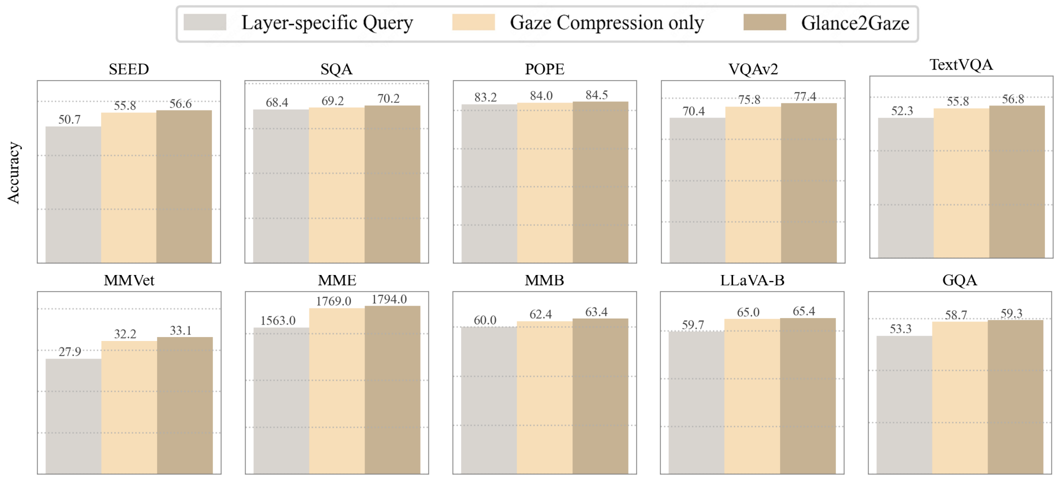

Figure 5: More ablation results on significance of shared query pool and the effect of Glance Fusion.

Table 9: Ablation studies on r and p_r, evaluated on VQAv2 dataset.

Method	p_r=256					r=9			
	r=1	r=3	r=9	r=17	r=25	p_r=32	p_r=128	p_r=256	p_r=529
FLOPs	12%	17%	33%	56%	78%	24%	28%	33%	42%
Acc	70.2	74.6	77.6	78.1	78.4	74.7	75.4	77.6	77.9

Figure 5. Adding Glance Fusion before Gaze Compression significantly improves performance across all datasets, with notable gains on fine-grained OCR tasks like TextVQA and VQAv2.

Ablation study on r and p_r. In Gaze Compression, the initial compression layer index r and the size of query embedding p_r together shape the compression ratio. To evaluate the performance impact of each variable independently, we varied one while holding the other constant, facilitating a comparative analysis of their effects, as shown in Table 9. It reveals a direct proportional relationship between accuracy and the starting compression layer when p_r is constant; larger r corresponds to higher accuracy. This is logical, as premature compression may prevent the LLM from fully processing visual tokens. Similarly, opting for a larger query embedding size yields benefits, as it allows richer information capture during compression.

Exploration on number of layers in Glance Fusion. We fuse different numbers of ViT layers, with results displayed in Figure 6 (a). Interestingly, adding more ViT layers does not always result in proportional performance gains. This aligns with observations in Figure 1, suggesting significant redundancy across layers and certain intermediate layers in ViT not contributing to instruction comprehension. To balance performance across all datasets, we selected 4 layers for fusion in this study.

Necessity of Instruction in Glance Fusion. To demonstrate the significance of instruction in Glance Fuse, we compared it with straightforward feature averaging across layers. As illustrated in Figure 6 (b), indiscriminate fusion of ViT layers results in minimal improvement, whereas instruction-guided fusion significantly enhances features and boosts performance.

A.3.4 More efficiency comparison

We provide comprehensive tables summarizing the training cost, inference latency, prefilling time, and throughput across different frameworks and compression configurations, offering a clear overview of the computational efficiency, as shown in Table 10.

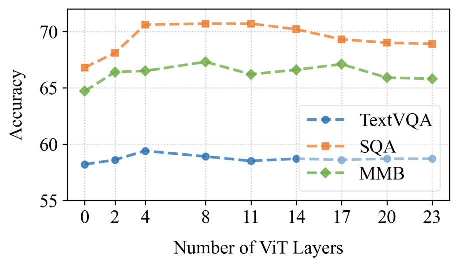

(a) Exploration on number of ViT layers

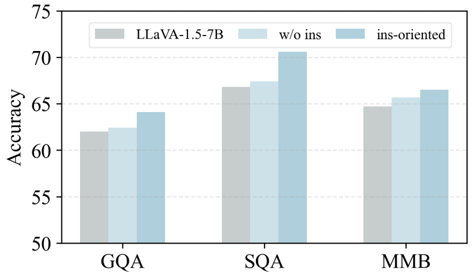

(b) Importance of Instruction-oriented integration

Figure 6: Ablation studies on Glance Fusion module.

Table 10: Comparison of computational efficiency between Glance2Gaze and baseline models. Metrics include training GPU hours, inference TFLOPs, latency, CUDA time, and throughput.

Method	**Training GPU Hours**	**Inference TFLOPs**	**Latency (ms)**	**CUDA Time (ms)**	**Throughput**
LLaVA-1.5-7B family					
LLaVA-1.5-7B	104	10.07	185.9	115	28.754
Glance2Gaze (33% FLOPs)	72	3.36	133.2	66	40.022
Glance2Gaze (22% FLOPs)	60	2.22	109.2	32	51.351
Glance2Gaze (11% FLOPs)	43	1.11	100.2	22	56.820
LLaVA-Next-7B family					
LLaVA-Next-7B	366	53.83	475.2	313	10.884
Glance2Gaze (22% FLOPs)	242	11.84	262.0	100	19.741
Glance2Gaze (11% FLOPs)	173	5.53	191.9	90	30.719
Glance2Gaze (5% FLOPs)	87	2.67	151.2	49	34.121
Video-LLaVA family					
Video-LLaVA	297	37.38	739.6	342.2	21.599
Glance2Gaze (6% FLOPs)	151	2.24	484.3	125.1	35.095